

Supplementary file 1

MicroRNA-372-3p impairs fatty acid metabolism in hepatocellular carcinoma cells by targeting *CPT1A* and *ACSL4*

Chinnatam Phetkong^{1,2,3}, Thammachanok Boonto^{2,3}, Pannathon Thamjamrassri^{2,3}, Chaiyaboot Ariyachet^{1,2,3*}, Pisit Tangkijvanich^{2,3}

¹Medical Science Program, Faculty of Medicine, Chulalongkorn University, Bangkok, 10330, Thailand

²Department of Biochemistry, Faculty of Medicine, Chulalongkorn University, Bangkok, 10330, Thailand

³Center of Excellence in Hepatitis and Liver Cancer, Faculty of Medicine, Chulalongkorn University, Bangkok, 10330, Thailand

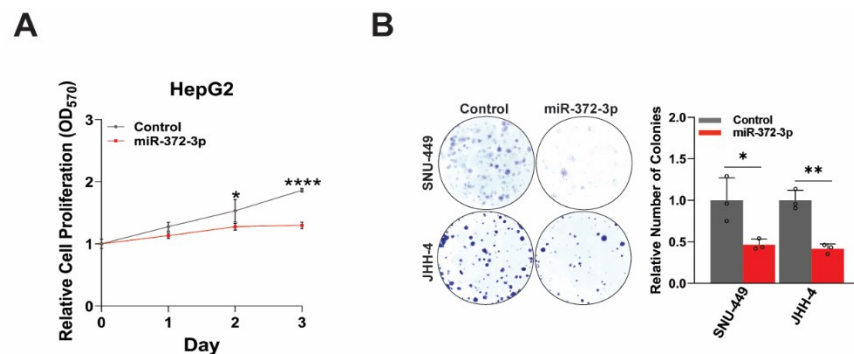


figure S1: Effects of miR-372-3p overexpression on HCC cell proliferation and colony formation. (A) MTT assay assessing the effect of miR-372-3p overexpression on HCC cell proliferation (n = 3). (B) Colony formation assay of control and 372-OE HCC cells, with representative images and quantification of colony numbers per well (n = 3). All experiments were quantified using Fiji software, normalized to the control group, and analyzed using Student's t-test. Data are presented as mean \pm SD, with significance levels indicated as * $p < 0.05$, ** $p < 0.01$, *** $p < 0.001$, and **** $p < 0.0001$.

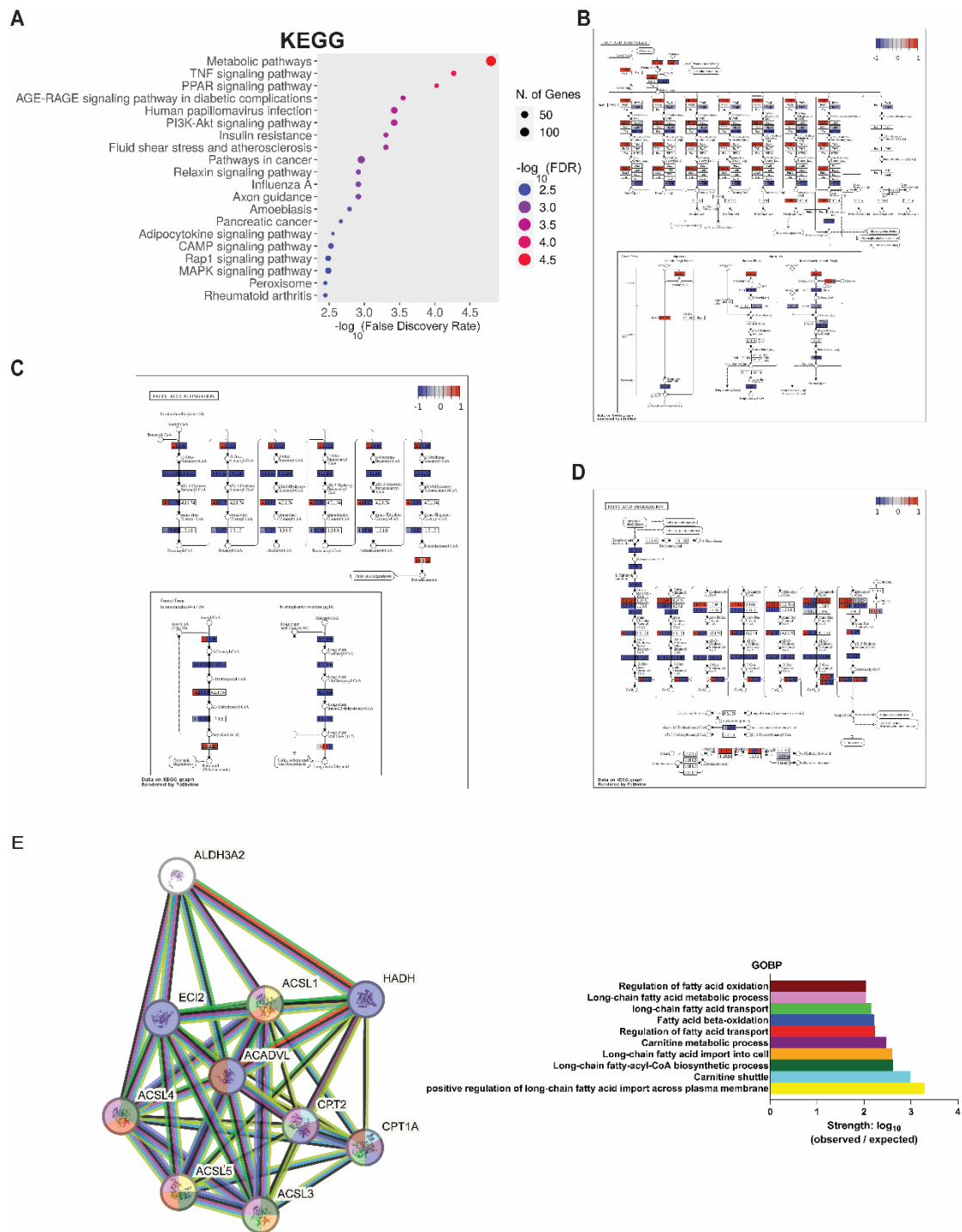


figure S2: Enrichment and network analysis of downregulated DEGs in fatty acid metabolism. (A) KEGG enrichment analysis of downregulated DEGs, with the Pathview analysis mapping DEGs onto KEGG pathways to illustrate expression patterns. Blue and red represent downregulated and upregulated genes, respectively. (B) Pathview analysis of downregulated DEGs in fatty acid

biosynthesis. (C) Pathview analysis of downregulated DEGs in fatty acid elongation. (D) Pathview analysis of downregulated DEGs in fatty acid degradation pathways. (E) STRING network analysis of ten core genes in fatty acid metabolism, analyzed using GOBP terms (left panel) and strength scores (FDR < 0.05, right panel).

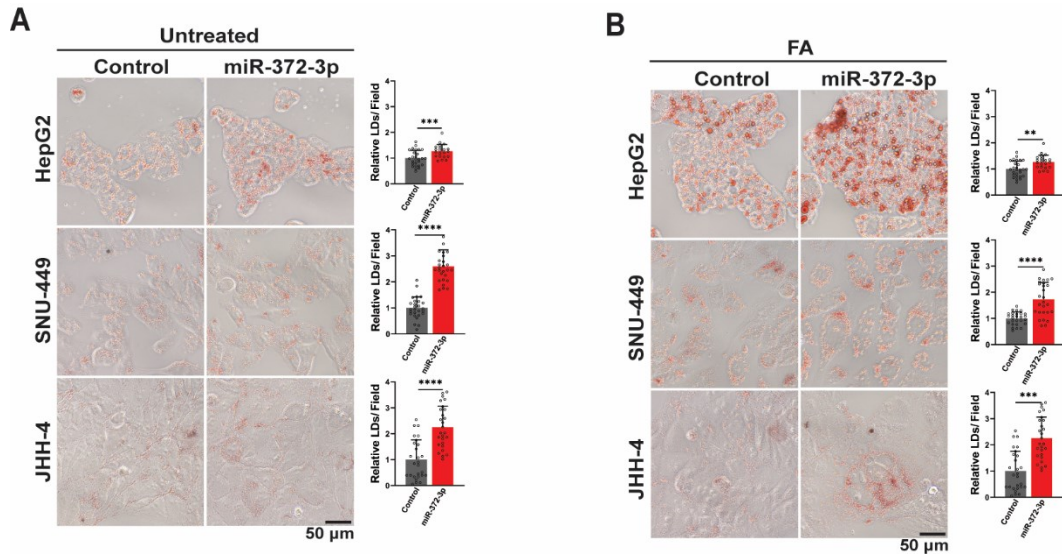


figure S3: Oil Red O (ORO) staining of control and 372-OE HCC cells under basal (A) and fatty acid (FA)-treated conditions (B), with representative images and quantification of lipid accumulation (n = 27). All experiments were quantified using Fiji, normalized to the control group, and analyzed using Student's t-test. Data are presented as mean \pm SD, with significance levels indicated as * $p < 0.05$, ** $p < 0.01$, *** $p < 0.001$, and **** $p < 0.0001$.

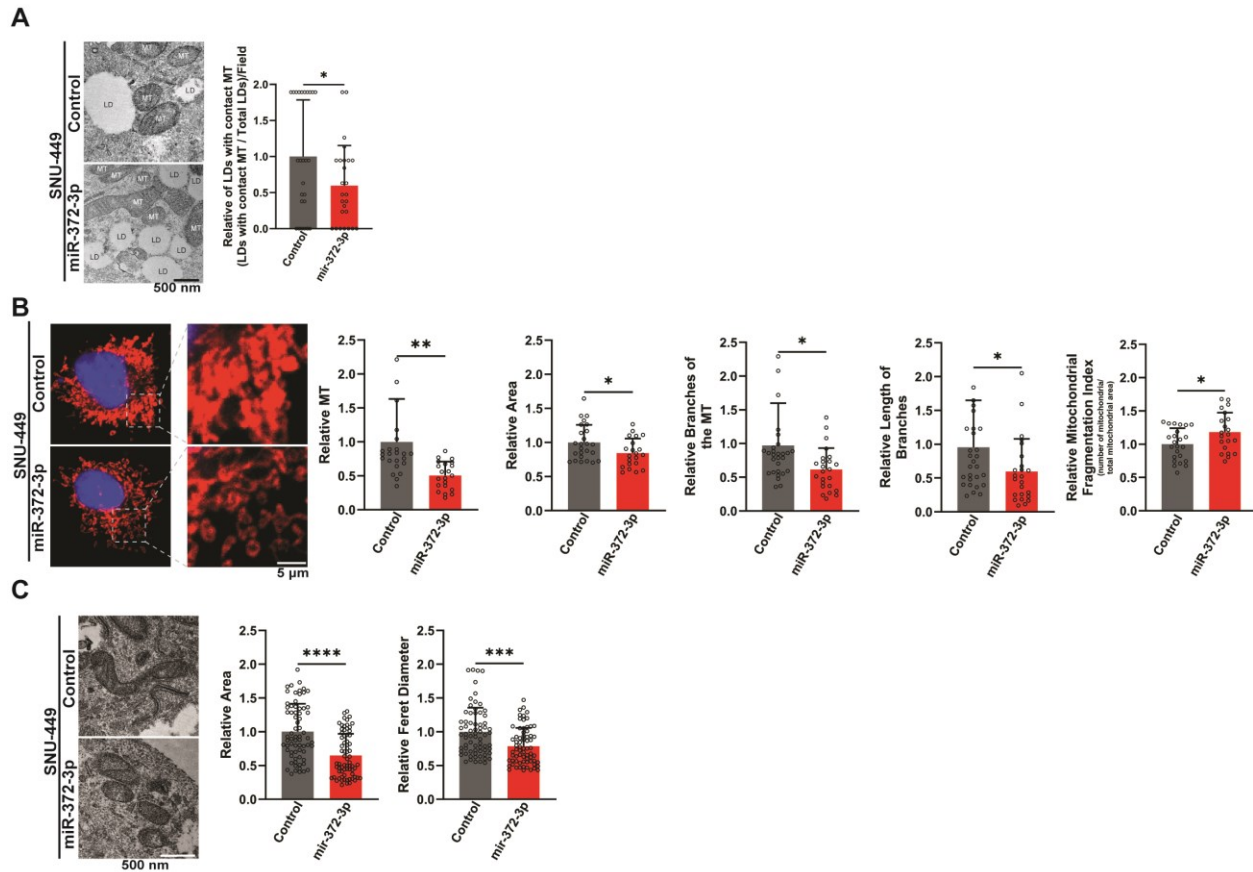


figure S5: Structural and morphological analysis of interaction between lipid droplets (LDs) and mitochondria (MT) and mitochondrial dynamics. (A) Analysis of LD-MT contact by transmission electron microscopy (TEM) micrographs showing LDs in contact with MT (left panel), with quantification of relative LD-MT contact per field (right panel, $n = 26$). (B) Confocal microscopy analysis of mitochondrial morphology maximum intensity projection (MIP) images illustrating mitochondrial fission in control and 372-OE HCC cells (left panel), with quantification of relative mitochondrial number and morphology (right panel, $n = 21-29$). (C) TEM analysis of mitochondrial structure with representative TEM micrographs showing mitochondrial structure (left panel), with quantification of relative mitochondrial areas and Feret diameter (right panel, $n = 65-70$). All experiments were quantified using EN 2.3 Lite and Fiji software, normalized to the control group, and analyzed using Student's t-test. Data are presented as mean \pm SD, with significance levels indicated as $*p < 0.05$, $**p < 0.01$, $***p < 0.001$, and $****p < 0.0001$.

Table S1: Primer sequences used in this study.

Primer	Sequence 5→3'
Cloning primers	
F_EcoRI_miR-372-3p	GCTGAATTCACCTTGCGATCGCCGCCTTG
R_BamHI_miR-372-3p	CGAGGATCCAGCCGCCCTCTGAACCTTC
Top_WT_3'UTR_CPT1A	CGCGGCCGCGGCTCATGCTACAGCGTCGTGAAAC
Bottom_WT_3'UTR_CPT1A	TCGAGTTTCACGACGCTGTAGCATGAGCCGCGGCCGCGAGCT
Top_MUT_3'UTR_CPT1A	CGCGGCCGCGAGTATTCAAGAAGCAACCAGCACCC
Bottom_MUT_3'UTR_CPT1A	TCGAGGGTGCTGGTTGCTTCTTGAATACTGCGGCCGCGAGCT
Top_WT_3'UTR_ACSL4	CGCGGCCGCGAGCAAAAGTGCTGCAGGGCTTTAC
Bottom_WT_3'UTR_ACSL4	TCGAGTAAAGCCCTGCAGCACTTTTGCTGCGGCCGCGAGCT
Top_MUT_3'UTR_ACSL4	CGCGGCCGCGAGCAAAAGTGCGCGTCGTGAAAC
Bottom_MUT_3'UTR_ACSL4	TCGAGTTTCACGACGCGCACTTTTGCTGCGGCCGCGAGCT
Top_WT_3'UTR_CPT2	CGCGGCCGCGAGCTGGGTGTGGTGGCATGC
Bottom_WT_3'UTR_CPT2	TCGAGCATGCCACCACACCCAGCTGCGGCCGCGAGCT
Top_MUT_3'UTR_CPT2	CGCGGCCGCGAGCTGGGTGTGCGTCGTGAAAC
Bottom_MUT_3'UTR_CPT2	TCGAGTTTCACGACGCACACCCAGCTGCGGCCGCGAGCT
Top_mir-372-3p_Silencer	GATCCACGCTCAAATGTGCGAGCACTTTCCACACCAAAGTGCTGCGACATTTGAG CGTTTTTTGGAAA
Bottom_miR-372-3p_Silencer	AGCTTTTCCAAAAAACGCTCAAATGTGCGAGCACTTTGGTGTGGAAAGTGCTGC GACATTTGAGCGTG
qRT-PCR primers	
F_U6	CTCGCTTCGGCAGCACAA
F_miR-372-3p	AGTGCTGCGACATTTGAGCG
R_universal_miR	CTCGCTTCGGCAGCACAA
F_CPT1A	GGTGTCTAAATATCTCGCTGTGG
R_CPT1A	GGACACGTA CTCTGGGTTATTC
F_ACSL4	CCAAAGAACACCATTGCCATC
R_ACSL4	AGCCTCAGATTCATTTAGCCC
F_CPT2	TTGAGTGCTCCAAGTACCATG
R_CPT2	GCAAACAAGTGTCGGTCAAAG
F_ECI2	GACAGGGCAACATTTCATAAC
R_ECI2	CCTCTCCCGCTGTAACTTC
F_RPL19	GCTCTTTCTTTTCGCTGCT
R_RPL19	CATTGGTCTCATTGGGGTCT